

# Assessment of Compressed-Sensing Reconstruction Fidelity for Depicting Ventilation Defects in Hyperpolarized He3 MRI using H1 Image-masked Segmentation

Kun Qing<sup>1</sup>, Nicholas J. Tustison<sup>2</sup>, Talissa A. Altes<sup>2</sup>, Jaime F. Mata<sup>2</sup>, G. Wilson Miller<sup>2</sup>, Eduard E. De Lange<sup>2</sup>, William A. Tobias<sup>3</sup>, Gordon D. Cates<sup>3</sup>, James R.

Brookeman<sup>2</sup>, and John P. Mugler, III<sup>1,2</sup>

<sup>1</sup>Biomedical Engineering, University of Virginia, Charlottesville, VA, United States, <sup>2</sup>Radiology and Medical Imaging, University of Virginia, Charlottesville, VA,

United States, <sup>3</sup>Physics, University of Virginia, Charlottesville, VA, United States

**Target audience:** Imaging scientists and physicians interested in hyperpolarized-gas MRI, accelerated imaging, and assessment of pulmonary function.

**Introduction & Purpose:** Combined acquisition of helium-3 (He3) and proton (H1) 3D image sets within one breath-hold can be accelerated using the compressed-sensing (CS) technique [1,2]. Direct and quantitative comparison of fully-sampled and CS images has been implemented separately for He3 and H1 acquisitions by incorporating the fully-sampled and undersampled He3 or H1 scans into a single breath-hold [3]. Undersampled, CS-reconstructed H1 images showed relatively high similarity to fully-sampled images. Both He3 and H1 images were found to have a low mean absolute percentage error (MAPE) and high structural similarity (SSIM) index as compared with simulated CS results [1]. Somewhat lower similarity indices were found for direct comparison of fully-sampled and CS He3 image sets, most of which appeared to be caused by factors unrelated to the CS technique such as diaphragm movement and the non-equilibrium nature of hyperpolarized magnetization. Considering that the major application of He3 ventilation imaging is to distinguish normally-ventilated areas from those with poor ventilation (ventilation “defects”), an automated segmentation method [4] was proposed recently for quantifying ventilation defects in He3 images using He3/H1 multivariate templates to register and segment the He3 images [5]. The purpose of this study was to compare and quantify the ventilation defects found in fully-sampled and CS-reconstructed undersampled He3 image sets acquired in the same subjects but during different breath-holds.

**Methods:** *Experimental setup:* Studies were performed at 1.5T (Avanto, Siemens) using a chest He3 RF coil (Rapid Biomedical). He3 gas was polarized by collisional spin exchange with an optically-pumped rubidium vapor using a custom-built system. Experiments were performed under a Physician’s IND for imaging with hyperpolarized He3 using a protocol approved by our institutional review board. Informed consent was obtained in all cases. Fully-sampled and undersampled (acceleration factor R=3) data sets were acquired in different breath holds in two asthmatics (S1 and S2) using the combined He3/H1 acquisition.

*Pulse sequences:* A 3D balanced steady-state free-precession pulse sequence (TrueFISP) was used for He3 acquisitions, while a 3D spoiled gradient echo pulse sequence was used for H1. Parameter settings included: He3: flip angle 9°, TR/TE 1.86/0.79 ms, matrix 128x72x44 (S1) or 128x88x60 (S2), bandwidth/pixel 1085 Hz; and H1: flip angle 10°, TR/TE 1.80/0.78 ms, matrix 128x100x56 (S1) or 128x120x72 (S2). Spatial resolution was 3.9x3.9x3.9 mm for all acquisitions. Total acquisition time was 5.4 s for S1 and 8.5 s for S2 at R=3, compared with 9.8 s for S1 and 15.7 s for S2 with full sampling. Undersampling patterns were generated using a MonteCarlo algorithm, as described by Lustig et al [2]. The Cohen-Daubechies-Feauveau 9/7 (CDF 9/7) wavelet was used as the sparsifying transform. All CS reconstructions were implemented in MATLAB(The Mathworks, Natick, MA).

*Registration and segmentation:* Four steps were followed: (1) All image sets were N4 bias corrected to eliminate signal intensity variation due to B1 inhomogeneity effects. (2) Whole-lung masks were generated for the fully-sampled and CS H1 image sets based on registration with an H1 image-labeled template generated from eight subjects’ H1 chest images. (3) The CS H1 image was registered to the fully sampled H1 image to provide the mapping of the undersampled He3 ventilation image to its counterpart acquired in the fully-sampled acquisition. (4) Lung regions were segmented into 4 regions based on signal intensities, with two of them (Label 1, 2) representing the poorly-ventilated regions and the other two (Label 3, 4) representing the normally-ventilated regions. Label overlays between the two segmented and labeled maps were measured using the Dice metric after combining the poorly-ventilated labels and the normally-ventilated labels. Registration and segmentation scripts are available under Advanced Normalization Tools (ANTs) package [6].

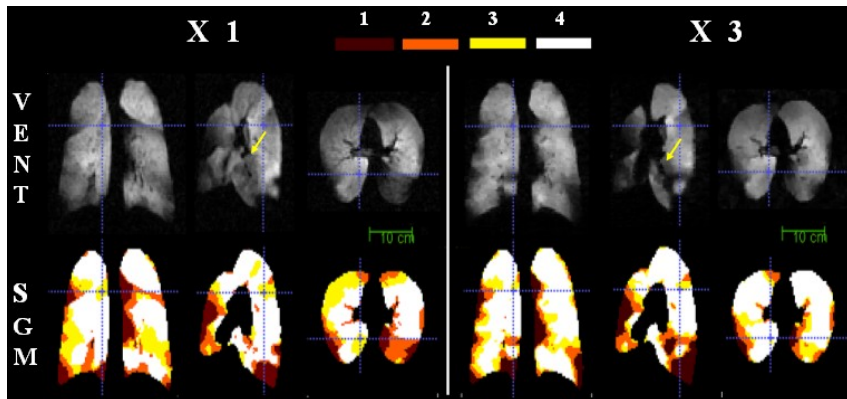


**Figure 1.** Fully-sampled (X1) versus CS (X3; R=3) acquisitions: Coronal, sagittal and axial He3 ventilation images are shown with the corresponding segmentation maps.

**Results and Discussion:** Means of the Dice metric of the overlaid labels are reported in Table 1 showing good agreement between the two segmentations. The mean Dice values calculated from Class 2, which corresponds to the normally-ventilated areas, are high -- both larger than 0.9. The mean Dice values obtained from Class 1, representing

**Table 1.** Label overlap between the fully-sampled and undersampled (R=3) acquisitions.

Subject		Subject	
		S1	S2
Mean Dice			
Total		0.85	0.78
Class 1(label 1,2)		0.80	0.76
Class 2(label 3,4)		0.95	0.91

poorly-ventilated regions, are lower. Reviewing the underlying ventilation images, this appears to be at least partly due to actual variations of the ventilation defects between breath holds (e.g., yellow arrows, Figures 1 and 2) rather than artifacts from the CS reconstruction. Figure 1 shows an example of 3-planes of both the fully-sampled and CS ventilation images, and the respective labeled segmentation maps from subject S2. The ventilation defects identified by segmentation are very close but not completely identical. Some defects appeared worse in CS images (yellow arrows, Figure 1) while others appeared worse in fully-sampled images (yellow arrows, Figure 2).

**Conclusions:** The automated segmentation methods described in [4] have been applied to quantitatively compare the undersampled, CS-reconstructed and fully-sampled datasets. Relatively high similarities were found between the segmentation results. Much of the difference appears to be due to real variation of ventilation defects between breath holds rather than artifacts related to the CS acquisition.

**References:** [1] Qing K et al. Proc ISMRM 19 (2011): 546. [2] Lustig M et al. Magn Reson Med 2007;58:1182. [3] Qing K et al. Proc ISMRM 19 (2012): 4003. [4] Tustison NJ. JMRI 2011; 34: 831. [5] Tustison NJ. Proc of SPIE Vol. 8672-33. [6] <http://www.picsl.upenn.edu/ANTs>. **Acknowledgement:** Supported by R01 HL097077 and Siemens Medical Solutions.

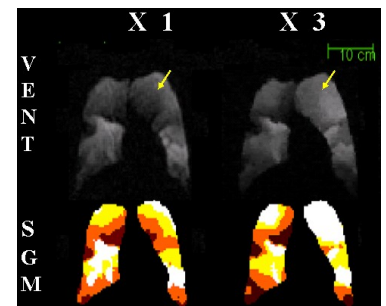


**Figure 2.** Coronal fully-sampled (X1) versus CS (X3; R=3) He3 ventilation images and corresponding segmentation maps.